Journal of Hazardous Materials, 36 (1994) 55–68
Elsevier Science Publishers B.V., Amsterdam

Mechanisms of metal stabilization in cementitious matrix: Transmission electron microscopic study of C_3A/CuO fixation system

Tzong-Tzeng Lin[a], Cheng-Fang Lin[a,*] and Wen-Cheng J. Wei[b]

[a] *Graduate Institute of Environmental Engineering, National Taiwan University, Taipei (Taiwan, R.O.C.)*
[b] *Institute of Materials Science and Engineering, National Taiwan University, Taipei (Taiwan, R.O.C.)*

(Received February 25, 1993; accepted in revised form April 10, 1993)

Abstract

A detailed understanding of the reaction mechanisms would be useful to predict and control the ability of fixation systems to retard the solubility and/or mobility of the incorporated metal species. For the present study, the interactions between tricalcium aluminate (C_3A) paste and CuO were characterized using transmission electron microscopy (TEM) equipped with energy-dispersive X-ray analysis (EDAX). The results of TEM/EDAX analyses indicated that the concentration gradient of copper species in the hydrated C_3A region and physical entrapment of CuO within five principal hydration products of C_3A were attributed to the interactions of hydrated C_3A and CuO. Additionally, no intermediate phases or new chemical products of copper related compounds existed in the five typical interfaces. No diffraction patterns of metal copper, CuO, $Cu(OH)_2$, and $CuCO_3$ compounds were observed in the hydrated C_3A. It was thus suggested that the CuO was stabilized in the C_3A paste by two major mechanisms; the heterogeneous solid solution of copper species was present in the hydrated C_3A and CuO was physically entrapped by the hydration products of C_3A.

1. Introduction

Solidification/stabilization (S/S) technology is a widely practiced, cost-effective means of reducing leachability of hazardous heavy metal from the disposed waste in landfills [1, 2]. Many S/S treatment processes utilize a monolithic matrix containing one or more cementing materials such as ordinary portland cement, kiln dust, fly ash, or other natural pozzolanics [3]. However, very little is known about the microstructural changes and long-term stability of these metal contaminants such as copper, cadmium, lead, chromium, mercury, and zinc within cement matrices. Due to the complexity of cement-like systems,

*To whom correspondence should be addressed.

SSDI 0304-3894(93)E0052-4

there is a poor fundamental understanding of reaction, interfering, and leaching mechanisms of solidified or stabilized metal wastes. Therefore, it is difficult to predict and control the long-term leaching behaviors of a treated metal waste in landfill.

More recently, many researchers studying the development of S/S formulas are of the opinion that a full understanding of the microanalysis of solidified/stabilized hazardous wastes is important if better S/S systems are to be designed [3–7]. Electron microscopy techniques, i.e. scanning electron and transmission electron microscopies equipped with energy dispersive X-ray analysis (SEM/EDAX and TEM/EDAX) are able to offer valuable information on the S/S mechanisms. Chemical information available from SEM/EDAX can offer the elemental composition of a phase; but identification of a single compound is fairly difficult. TEM/EDAX can overcome some of these limitations and can give much higher resolution on localized information [3, 4]. Because the cementitious materials are usually fragile, it is difficult to prepare TEM/EDAX electron-transparent specimens (<100 nm). In this study, adequate specimens are specially prepared by an ultramicrotomy process for this purpose, so that the TEM/EDAX technique can be employed on the solidified matrix.

In recent studies [8–10], we have demonstrated how X-ray diffractometry (XRD) and SEM/EDAX can be successfully utilized to investigate the reaction mechanisms of CuO solidified by tricalcium aluminate ($3CaO{\cdot}Al_2O_3$, abbreviated as C_3A), tricalcium silicate ($3CaO{\cdot}SiO_2$, C_3S), and dicalcium silicate ($2CaO{\cdot}SiO_2$, abbreviated as C_2S). Although the SEM/EDAX microanalysis in sandwich sample (the lamination composed of three slices of cement constituent paste, CuO, and Cu materials) is able to observe a better interfacial morphology, the SEM micrographs only appear at the interface between overall hydration products of cement constituent and CuO. Therefore, the objective of this work is to provide detailed information of the microstructure and microchemistry of CuO solidified by C_3A fixing agents. Particular emphasis is placed on interfacial microanalysis for the major hydration products of C_3A paste and CuO by TEM/EDAX.

2. Materials and methods

2.1. Material

All the chemicals used in this work were reagent-grade products. C_3A was prepared by initially mixing with a 3:1 mole ratio of calcium carbonate (Cerac, 99.95% purity) and fused silica (99.9% purity, Harrison–Walker Refractories). The mixture was homogenized in a ball mill by adding anhydrous alcohol, allowed to dry at 85 °C for two hours, calcined at 950 °C for another two hours, then sintered at 1350 °C for 5 hours, followed by air quenching. The presence of C_3A was confirmed by XRD. CuO (Gredmann, 99.9% purity, Taiwan) as a model waste was used to represent a standard waste composition of Cu-bearing sludge and/or industrial or municipal incineration wastes.

2.2. Sample preparation

The solidified C_3A/CuO sample was prepared first by completely mixing equal weights of C_3A and CuO. Water was then added based on a water/solids (solid matter contains both of C_3A and CuO powder) weight ratio of 0.4 to carry out the hydration and/or other relevant reactions. The solidified sample was cured at 25 °C under a well humidified environment for 28 days. The technique of ultramicrotomy offers the best possibility to prepare successful specimens from solidified matrix with poor mechanical properties. The microtomed sample for TEM/EDAX was prepared using the solidified C_3A/CuO sample. The matrix was polished and the 100 μm slice was embedded in G-1 epoxy (Gatan, Inst. Co., USA). The embedding mixture formulation included one part of hardener and ten parts of resin. After having cured on a hot plate for two hours at 60 °C, the epoxy-mount sample was trimmed to a trapezium. The thin section was cut using a diamond knife to approximately 50 to 100 nm thick using a microtomer (LKB Noba ultramicrotomer) operated at a speed of 1 mm/s.

2.3. Analysis

The thin sections were put on a copper grid and coated with thin carbon film for TEM observations using a TEM (JEOL 100 CX II) operated at 100 kV and a TEM (JEOL 2000 FX analytical electron microscopy) equipped with a Link System 10000 EDAX operated at 160 kV. The TEM/EDAX analyses were performed by using bright field (BF) images, selected area diffraction (SAD), centred dark field (CDF), and micro-beam EDAX examinations (electron beam diameter, 0.05 μm) techniques. BF is the most commonly used imaging mode for crystalline materials. SAD is useful for identifying and/or determining the orientation of features of interest in specimens. The main advantage of CDF image observation is its high contrast. Furthermore, CDF image using specific diffraction spots is a very important and useful technique in analysing complicated diffraction patterns and in performing quantitative analyses of crystal defects. Because the micro-beam diameter is 50 nm or even less, the result of micro-beam EDAX analysis can minimize the effect of electron scattering.

3. Results and discussion

The TEM/EDAX work in this study is mainly exploited as an aid to further the understanding of interfacial microstructure and microchemistry between the major hydration products of C_3A paste and CuO. In the past studies, the results of the qualitative XRD patterns for C_3A/CuO solidified matrix have stated that the major hydration products were calcium aluminum hydroxide ($3CaO{\cdot}Al_2O_3{\cdot}6H_2O$, abbreviated as C_3AH_6), calcium aluminum oxide carbonate hydrate ($3CaO{\cdot}Al_2O_3{\cdot}CaCO_3{\cdot}11H_2O$, abbreviated as $C_3A\underline{C}H_{11}$), $CaCO_3$, and gibbsite (γ-$Al_2O_3{\cdot}3H_2O$, abbreviated as γ-AH_3) [8]. Therefore in the work here, five principal interfacial morphologies (C_3AH_6/CuO, $C_3A\underline{C}H_{11}$/CuO, C_3AH_{8-12}/CuO, CaO/CuO, and γ-AH_3/CuO) in the microtomed specimens are examined in terms of TEM micrographs.

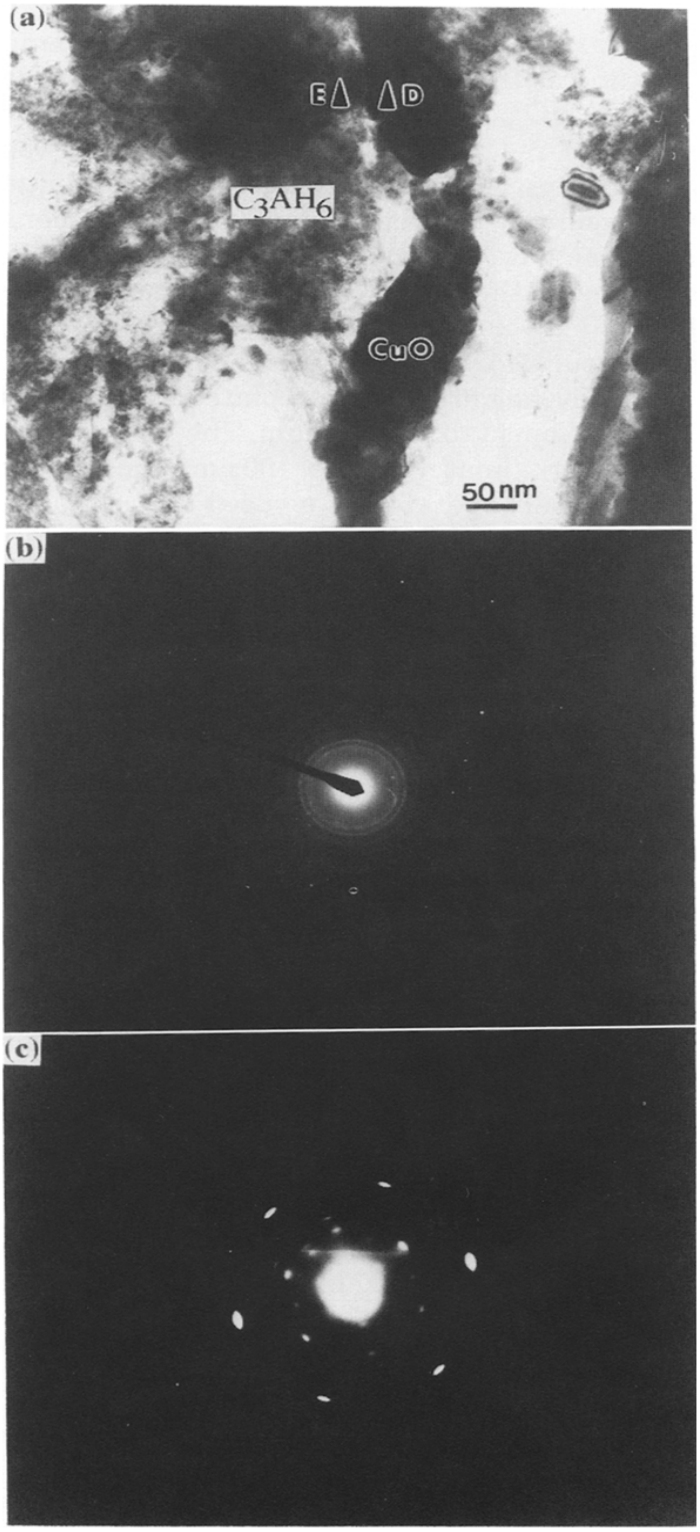

Fig. 1. (a) TEM bright-field image showing the interface of C_3AH_6 and CuO and the regions D and E analyzed by micro-beam EDAX; (b) and (c) SAD patterns of the CuO and C_3AH_6 region, respectively.

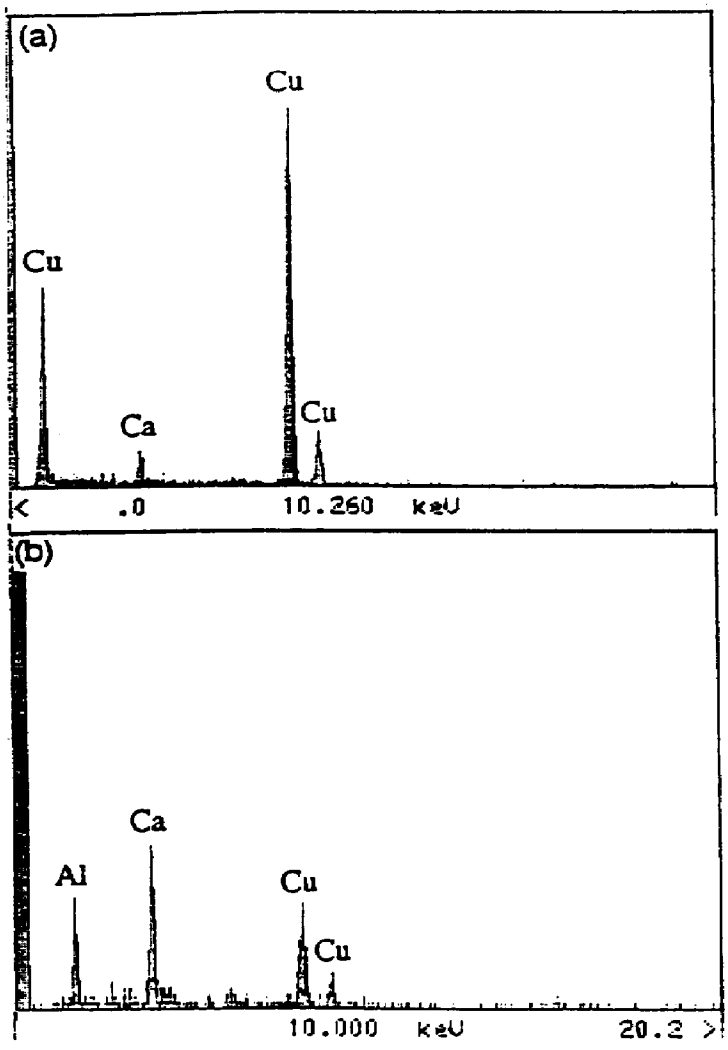

Fig. 2. (a) and (b) EDAX spectra of regions D and E pointed out in Fig. 1(a).

Figure 1(a) shows a typical interface of C_3AH_6 with some γ-AH_3 and CuO where CuO is entrapped by C_3AH_6 with no intermediate layer. The SAD diffraction patterns taken on both sides of the interface indicate only the presence of CuO and C_3AH_6 (Figs. 1(b) and 1(c), respectively). As C_3AH_6 is a major hydration product of C_3A paste, these two figures demonstrate that no reaction product between the two regions is observed. C_3AH_6, in all cases, appears in the cubic structure, with lattice parameter $a = 1.257$ nm. CuO shows a monoclinic structure, with lattice parameters $a = 0.468$ nm, $b = 1.097$ nm, $c = 0.576$ nm, and $\beta = 99.28°$. Two micro-beam EDAX spectra taken from regions D and E of Fig. 1(a) are shown in Figs. 2(a) and 2(b). The EDAX spectra clearly indicate the presence of Ca, Al, and Cu in the C_3AH_6 region and that the copper concentration decreases from the CuO side to the C_3AH_6 region. The change in copper concentrations across the interface might reveal that copper species diffuse into the C_3AH_6 region.

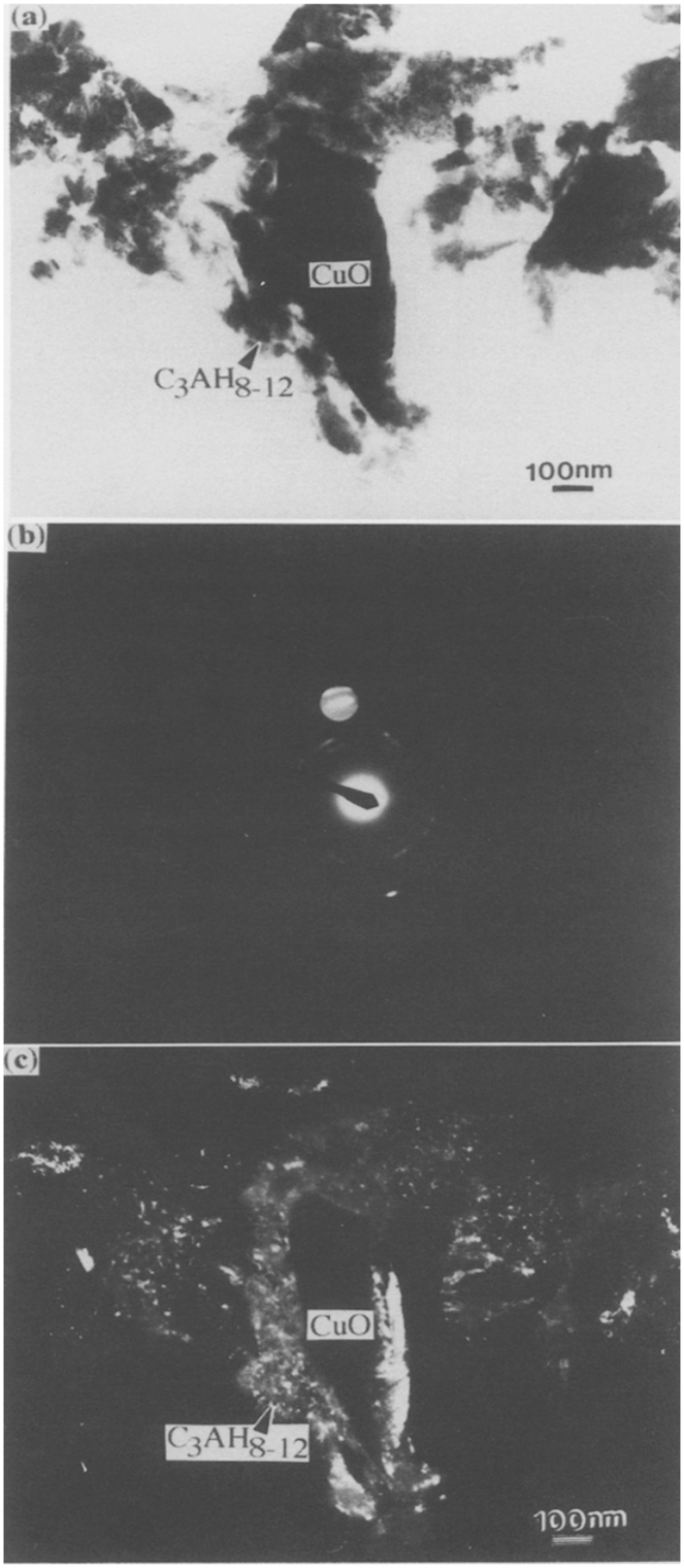

Fig. 3. (a) TEM micrograph of the interface of C_3AH_{8-12} and CuO; (b) SAD patterns of the C_3AH_{8-12} region; (c) the CDF image made by the fourth ring diffracted beam.

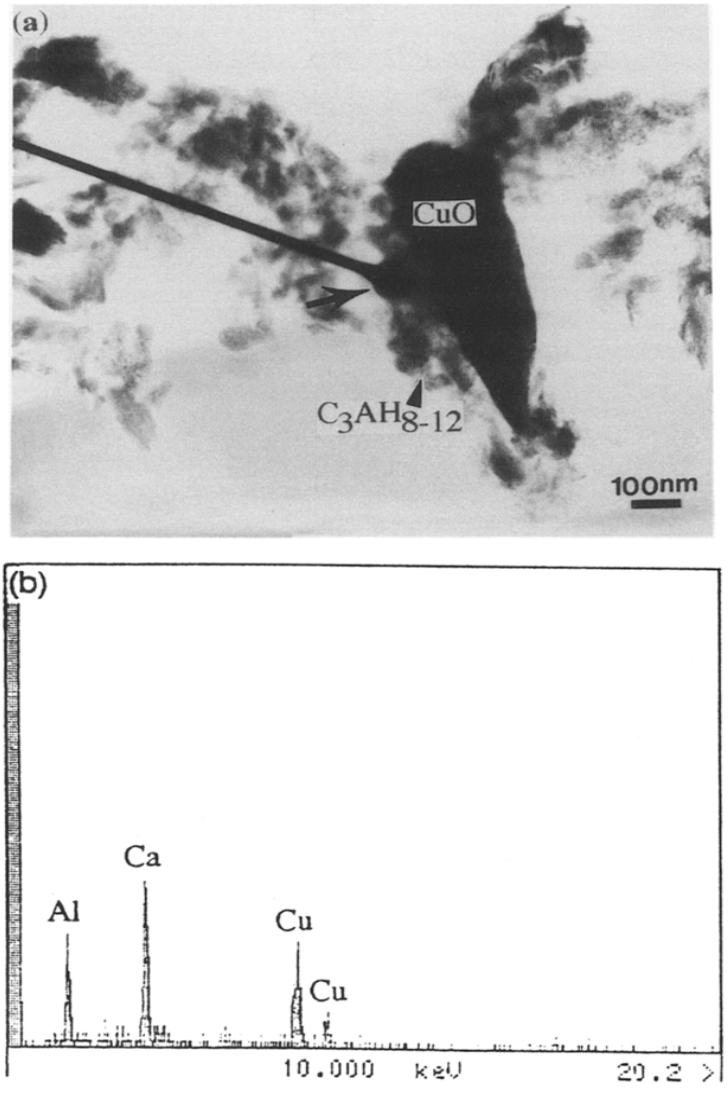

Fig. 4. (a) TEM micrograph showing the place analyzed using the micro-beam EDAX technique; (b) EDAX spectrum from the area pointed out by the arrow in Fig. 4(a).

The second interface examined is C_3AH_{8-12} and CuO. It appears from Fig. 3(a) that CuO grain is well entrapped by C_3AH_{8-12}. Figure 3(b) shows the ring diffraction patterns of double exposure on C_3AH_{8-12}. These ring patterns coincide well with that of the data file of the Joint Committee on Powder Diffraction Standards (JCPDS), pattern number: 2-83 for C_3AH_{8-12}. A CDF image (Fig. 3(c)) is made by allowing the diffracted beam of the fourth ring pattern pointed out in Fig. 3(b) and intercepting the transmitted beam. The CDF image can provide a very sharp boundary between C_3AH_{8-12} and CuO. From the figure, it is observed that no reaction product emerges in the interface. The locus analyzed using the micro-beam EDAX technique is pointed out

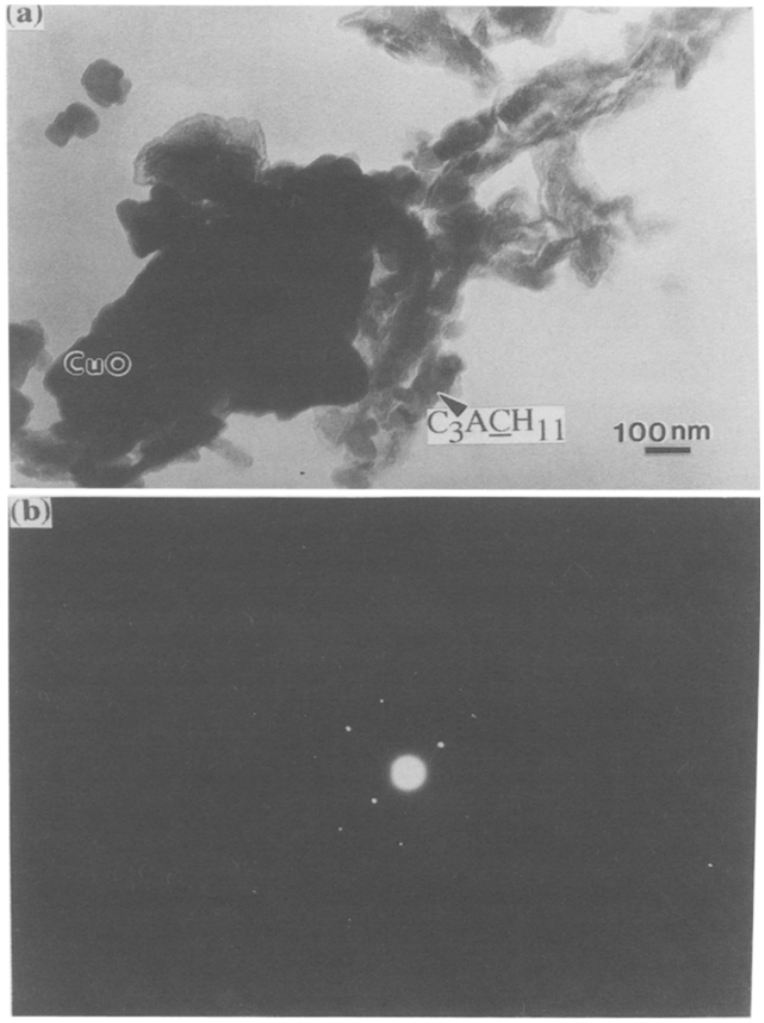

Fig. 5. (a) Micrograph of the interface of $C_3A\underline{C}H_{11}$ and CuO; (b) diffraction patterns from the vicinity of the interface among $C_3A\underline{C}H_{11}$, interface, and CuO regions.

by an arrow in Fig. 4(a) and the result is presented in Fig. 4(b). It can be shown from Fig. 4(b) that the presence of copper in the C_3AH_{8-12} region might imply the diffusion of copper species from CuO.

The third interface examined is $C_3A\underline{C}H_{11}$ and CuO which is shown in Fig. 5(a). As shown in Fig. 5(a), $C_3A\underline{C}H_{11}$ has contact with copper grain. The ring and spot patterns of SAD analysis on the interface of $C_3A\underline{C}H_{11}$ and CuO are shown in Fig. 5(b). The result reveals that the ring pattern is CuO and the spot pattern is the pseudohexagonal structure of $C_3A\underline{C}H_{11}$. The CDF images of both $C_3A\underline{C}H_{11}$ and CuO regions are shown in Figs. 6(a) and 6(b), respectively. It is very helpful to understand the interfacial changes by observing the overlap of the two CDF images. The result shows a very sharp boundary between the two phases with no new phase being observed. These figures

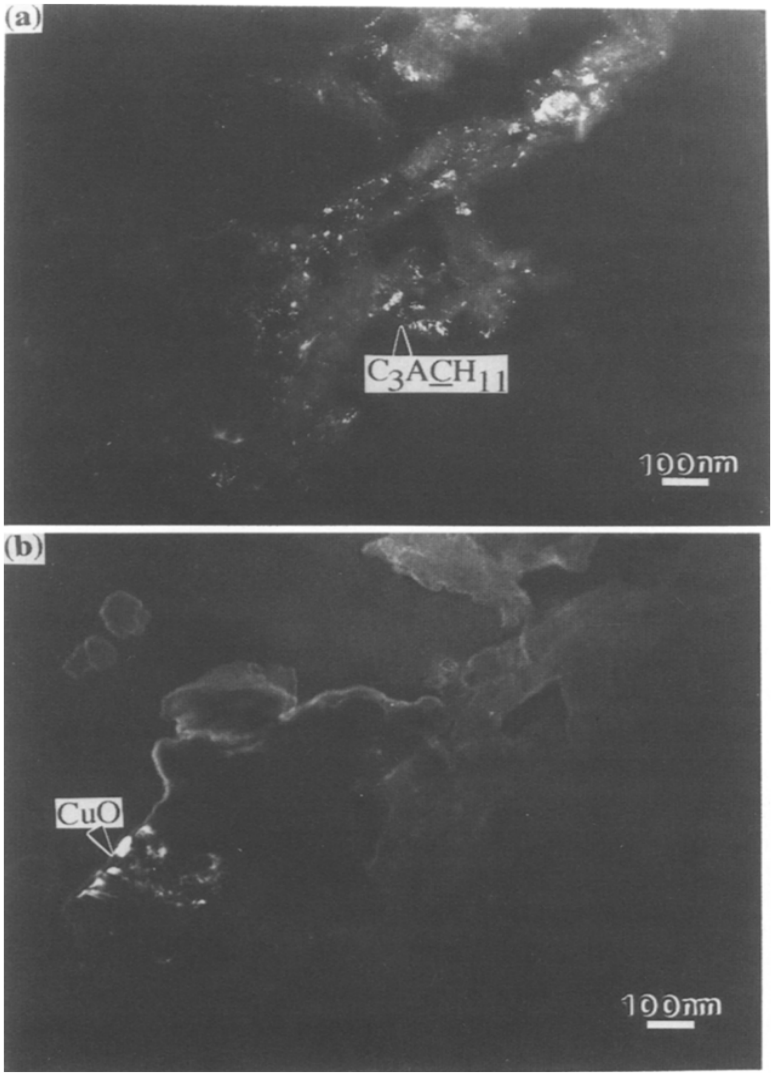

Fig. 6. (a) and (b) CDF images of $C_3A\underline{C}H_{11}$ and CuO produced by the diffracted beam of the ring and spot patterns, respectively.

clearly illustrate that no reaction product is formed between $C_3A\underline{C}H_{11}$ and CuO.

The CaO/CuO interface depicted in Fig. 7(a) shows that the likely interphase region between CaO and CuO is about 0.2 μm thick. The targeted interphase region (pointed out by the arrow in Fig. 7(b)) analyzed by using the micro-beam EDAX technique shows the presence of Ca and Cu (Fig. 7(c)). It is thus inferred that the interphase is formed by the reaction of CaO and CuO. The result of the SAD patterns taking on among three regions of CaO, the targeted interphase, and CuO is shown in Fig. 8(a), and results can be grouped into two sets of patterns: the ring pattern is the CaO phase (JCPDS pattern number: 4-777 for CaO); the spot pattern is the CuO phase (JCPDS pattern number: 5-661 for

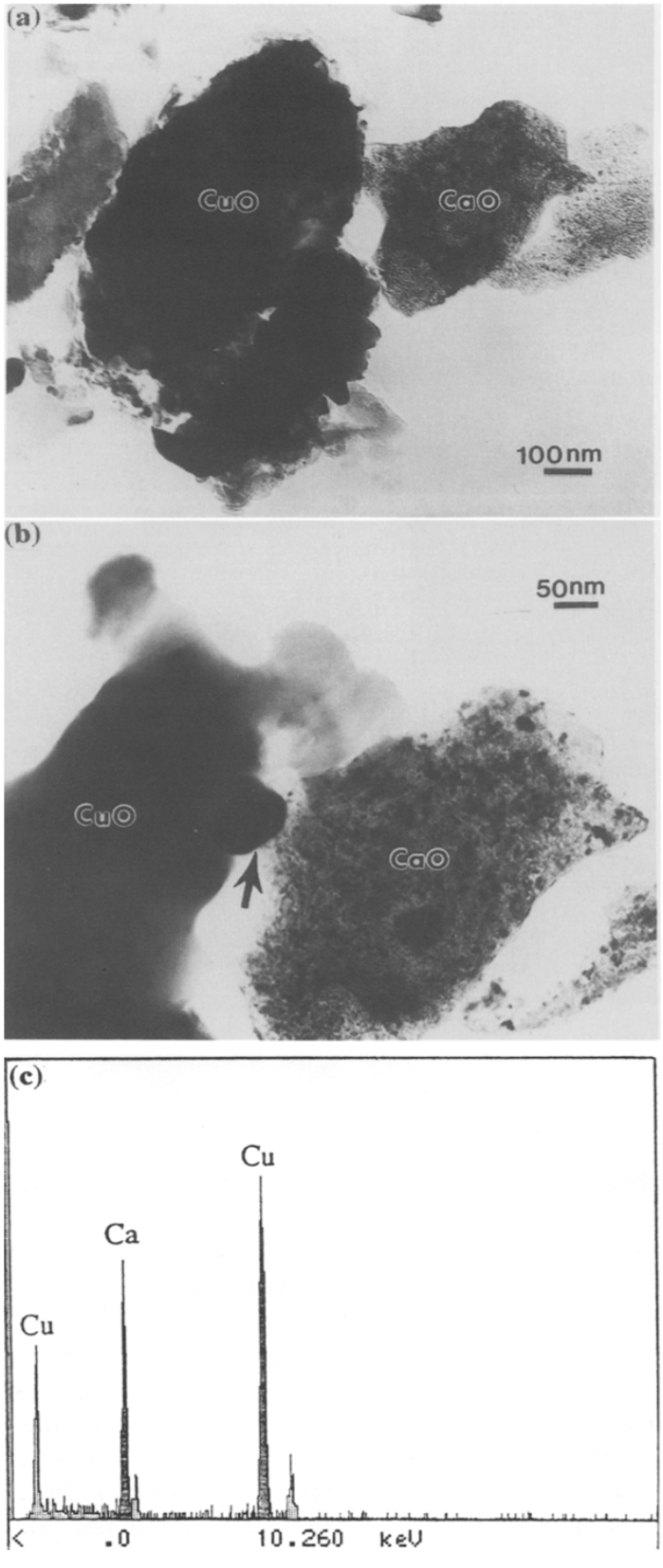

Fig. 7. BF micrograph of (a) the CaO/CuO interface and (b) the place analyzed using the microbeam EDAX technique; (c) EDAX spectrum from the area indicated by the arrow in Fig. 7(b).

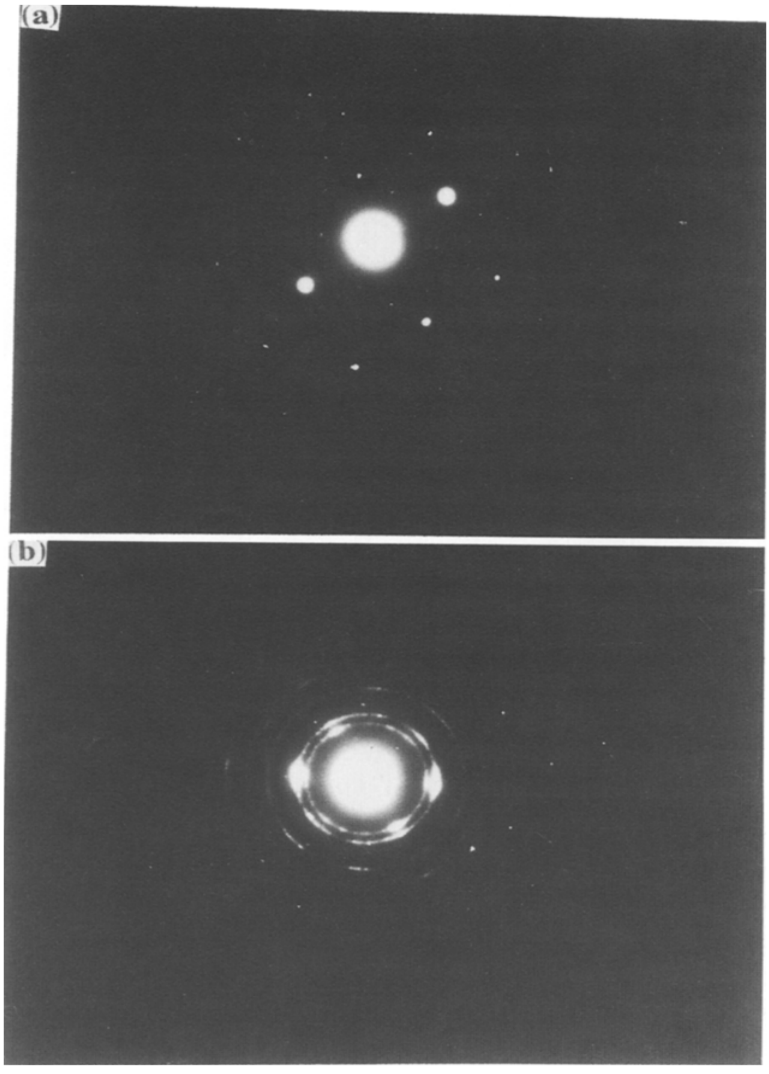

Fig. 8. SAD patterns from (a) the likely interphase and (b) CaO regions.

CuO). Moreover, SAD analyses on CaO (Fig. 8(b)) and CuO regions respectively reveal pure CaO and CuO phases. These results from SAD analyses on the targeted interphase are important evidences which might be used to draw the conclusion that no reaction product is found. Due to the fact that the copper species was exactly present outside the copper grain, it is thus suggested that the CaO region may consist of the diffused copper species.

The last interface examined is γ-AH_3 and CuO which is shown in Fig. 9. In the figure it obviously appears that CuO grains are well entrapped by γ-AH_3 materials. No significant difference between interface and matrix was observed in morphologies of γ-AH_3 and CuO. Results of micro-beam EDAX spectra taken on three different regions (as pointed out in Fig. 9) are shown in

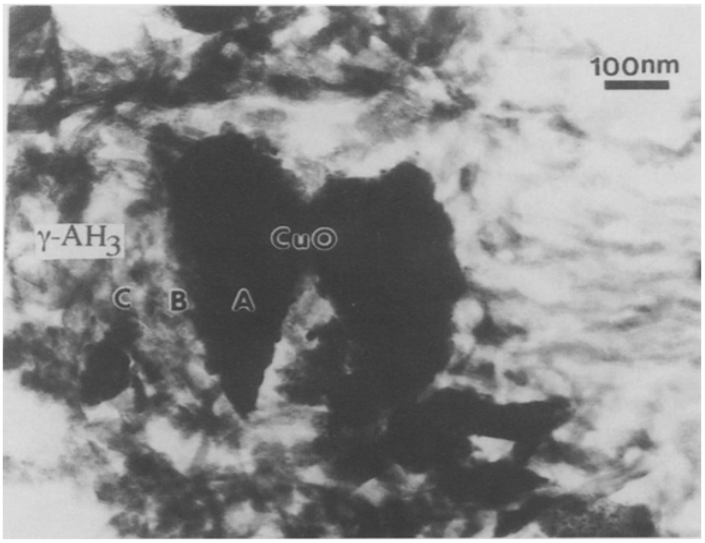

Fig. 9. (a) BF image of the interface of γ-AH_3 and CuO showing the regions A, B, and C for micro-beam EDAX analyses.

Figs. 10(a–c). This result clearly reveals that there is a concentration gradient of copper element in the γ-AH_3 region. Because of the diffusion of copper species into the γ-AH_3 region, the solid solution of copper species might exist in the γ-AH_3 region [8].

The results presented in Figs. 1–10 can be summarized as follows. Significant amounts of copper element are present in each hydration product region of C_3A paste. No distinguishable crystalline copper compound is found with different hydration products of C_3A. No intermediate phases or new chemical products of copper-related compounds exist in the typical interfaces. The TEM/EDAX results strongly support those of SEM/EDAX analyses in an earlier study [8] where the interaction zone between hydrated C_3A and CuO very likely can be presented as a solids solution of copper species. A heterogeneous solids solution may form in metastable equilibrium, in which each crystal layer as it forms is in distribution equilibrium with the particular concentration of the aqueous solution existing at that time [11]. Correspondingly, there will be a concentration gradient in the solid phase from the center to the periphery. Heterogeneous arrangement of copper species within the lattice is very likely, and as a result no diffraction patterns by TEM can be obtained. However, in reality a concentration gradient of copper species does appear in the differently hydrated C_3A region. Thus, we suggest that the copper species are acting as a solute which dissolves and diffuses in the solid hydration products of C_3A (as solvent) to form a heterogeneous solids solution whilst CuO is physically encapsulated within the hydration products of C_3A. These are the likely processes for the reaction mechanisms of C_3A paste and CuO.

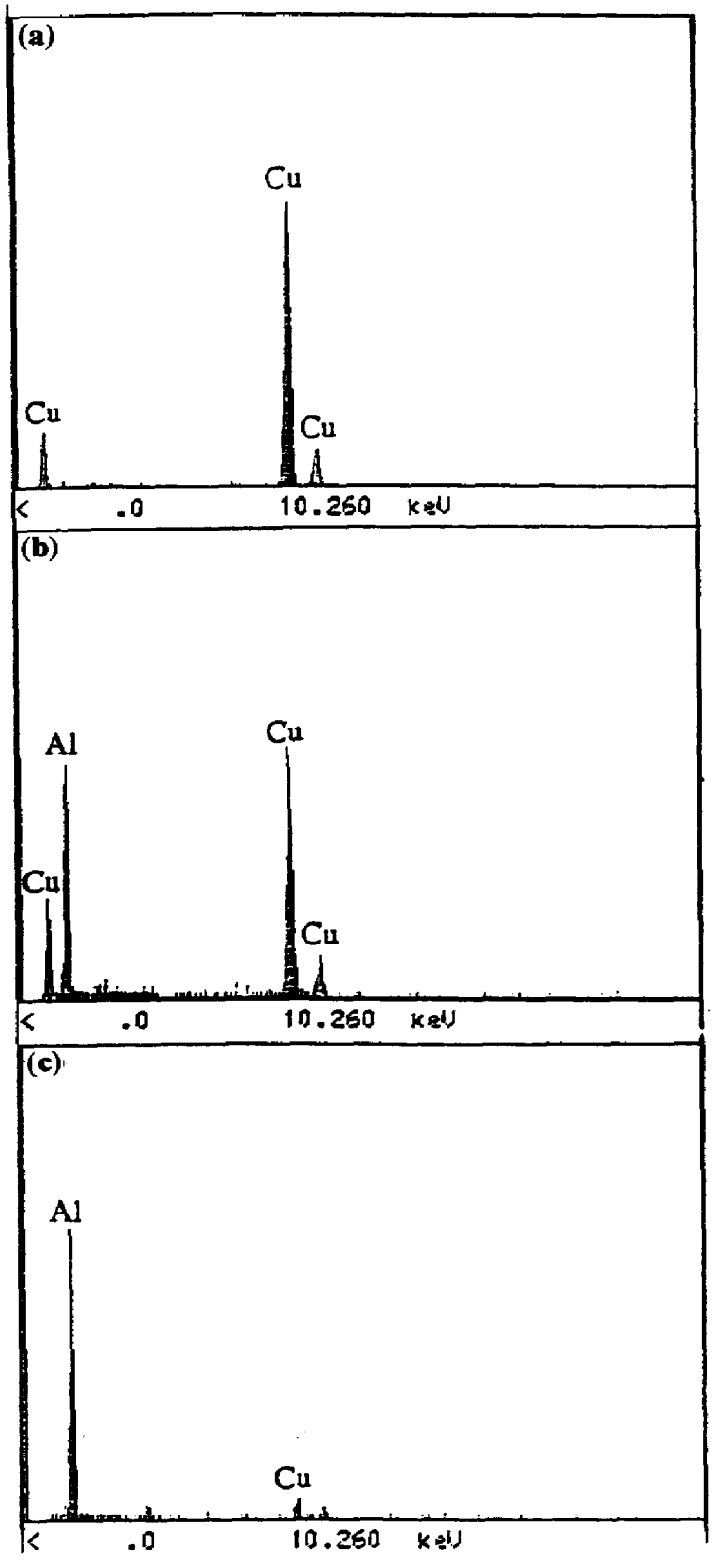

Fig. 10. EDAX spectra from the regions (a) A, (b) B, and (c) C as pointed out by the arrow in Fig. 9.

4. Conclusion

The TEM/EDAX microanalytical data observed from the by-microtome-excised specimen indicated that five principal hydration products (C_3AH_6, $C_3A\underline{C}H_{11}$, C_3AH_{8-12}, CaO, and γ-AH_3) of C_3A paste co-diffused with copper species and that the CuO grain was well entrapped in these hydration products. Because a concentration gradient of copper species existed in different hydration products of C_3A, no intermediate phases or new chemical products of copper-related compounds were presented at the five typical interfaces, and no diffraction patterns of metal copper, CuO, $Cu(OH)_2$, and $CuCO_3$ compounds were observed in the hydrated C_3A, these dissolved copper species might diffuse and bind in solid hydration products of C_3A to form a heterogeneous solids solution. It was thus suggested that the reaction mechanisms of C_3A/CuO fixation system consist of the formation of a heterogeneous solids solution of copper species in the hydrated C_3A and physical entrapment of CuO within the hydration products of C_3A. This work on cement constituent C_3A has provided a micro-scale observation of the reaction mechanisms of a model S/S process. The results would be very significant for understanding and predicting the long term stability of solidified waste matrix and will be helpful for future work on the interactions between other fixing agents and metal wastes.

Acknowledgements

This study was funded by the National Science Council of R.O.C. under contract No: NSC 81-0421-E-002-10-Z.

References

1 J.R. Conner, Chemical Fixation and Solidification of Hazardous Wastes, Van Nostrand Reinhold, New York, 1990.
2 R. Soundararajan, J. Hazardous Mater., 30 (1990) 199–212.
3 A.C. Chou, H.C. Eaton, F.W. Cartledge and M.E. Tittlebaum, Hazard. Waste Hazard. Mater., 5 (1988) 145–153.
4 D.G. Ivey and R.B. Heimann, J. Mater. Sci., 25 (1990) 5055–5062.
5 D.G. Ivey and M. Neuwirth, Cem. Concr. Res., 19 (1989) 642–648.
6 F.K. Cartledge, L.G. Bulter, D. Chalasani, H.C. Eaton, F.P. Frey, E. Herrera, M.E. Tittlebaum and S.L. Yang, Environ. Sci. Technol., 24 (1990) 867–873.
7 D.L. Cocke, M. Mollah, A. Yousuf, J.R. Parga and J.D. Ortego, J. Hazardous Mater., 30 (1992) 83–95.
8 T.T. Lin, C.F. Lin, W. Wei and S.L. Lo, Environ. Sci. Technol., (1993) in press.
9 T.T. Lin, C.F. Lin and W. Wei, Toxicol. Environ. Chem., (1993) in press.
10 T.T. Lin, C.F. Lin and W. Wei, Toxicol. Environ. Chem., (1993) in press.
11 W. Stumm and J. Morgan, Aquatic Chemistry, 2nd edn., Wiley-Interscience, New York, 1981.